Redondo Foj, MB.; Ortiz Serna, MP.; Carsí Rosique, M.; Sanchis Sánchez, MJ.; Culebras, M.; Gómez, CM.; Cantarero, A. (2015). Electrical conductivity properties of expanded graphite polycarbonatediol polyurethane composites. Polymer International. 64(2):284-292. doi:10.1002/pi.4788.

Electrical conductivity properties of expanded Graphite–Polycarbonatediol Polyurethane composites

B. Redondo-Foj[a], P. Ortiz-Serna[a], M. Carsí[a], M. J. Sanchis[a*], M. Culebras[b], C.M. Gómez[b] and A. Cantarero[b]

Abstract

Conductive polymer composites of segmented polycarbonatediol polyurethane (PUPH) and expanded graphite (EG) have been synthesized with different amounts of EG conductive filler (from 0 to 50 wt%). SEM, X-ray diffraction measurements, FTIR and Raman Spectroscopies demonstrated a homogeneous dispersion of the EG filler in the matrix. The dielectric permittivity of the composites showed an insulator to conductor percolation transition with the increase of the EG content. Significant changes in the dielectric permittivity take place when the weight fraction of EG is in the range of 20–30 wt%. Special attention has been paid to the dependence of the conductivity with the frequency, temperature and EG content. The addition of expanded graphite to the matrix causes a dramatic increase in the electrical conductivity of ten orders of magnitude, which is an indication of percolative behavior. A percolation threshold of ~30 wt% was evaluated by using the scaling law of the percolation theory.

Keywords: electrical conductivity; polyurethane; expanded graphite; broadband dielectric spectroscopy

[*]*Correspondence to: M. J. Sanchis, Departamento de Termodinámica Aplicada, Instituto de Tecnología Eléctrica, Universitat Politècnica de Valencia, Camino de Vera s/n, 46022 Valencia, Spain. E–mail: jsanchis@ter.upv.es*

[a]*Departamento de Termodinámica Aplicada, Instituto de Tecnología Eléctrica Universitat Politècnica de Valencia, Camino de Vera s/n, 46022 Valencia, Spain*

[b]Materials *Science Institute, University of Valencia, P.O. Box 22085, 46071 Valencia, Spain*

INTRODUCTION

Composites are a class of engineering materials consisting of a mixture of two or more components present as separated phases and combined to improve a given property of each individual component.[1-2] The conducting polymer–based composites are materials formed by a randomly fine dispersed conducting component (filler) in an insulating polymer matrix. In the recent years, there has been a growing interest in this type of materials due to their significant importance in both applied and basic sciences. These composites offer the possibility of manufacturing light materials with adequate mechanical properties, combining the inherent processability of polymers with the electrical conductivity of the filler–conducting constituent. They can be used, for example, as batteries, sensors, or Solar Cells.

Polycarbonatediol polyurethanes are very useful coatings for materials that are subjected to environmental and thermal degradation. The materials used in coating applications have to fulfill certain properties such as: high impact resistance, high elasticity, resistance to corrosion, sunlight, oxidation or weather conditions. The elastomeric-thermoplastic nature of the segmented polyurethanes make these materials ideal for coatings applications.[3,4] Another important property for coatings is the electrical conductivity. Conductive metals lack of properties such as elasticity and corrosion resistance. Carbon materials, such as carbon nanotubes (CNTs), have been used to increase the electrical properties of polymer matrices.[5] However, CTNs are very expensive for large-scale applications. Other conductive fillers such as graphite and its variants are being used to provide electrical conductive properties to polymeric matrices.[6,7] We expect to obtain a composite material based on polycarbonatediol

polyurethane as polymer matrix (PUPH) with excellent mechanical[8] (PUPH-matrix) and electrical properties (EG-filler), for possible coating applications.

A polymer matrix is basically an electrical insulating material due to the low concentration of free charge carriers. When a conducting constituent is added, new contributions can be presented. Their electrical response is mainly associated with relaxation phenomena occurring under the influence of the alternated current (ac). The ac electrical response of disordered systems to electric perturbations results in the superposition of different contributions.[9,10] These contributions are related to: (i) the hopping process of localized charge carriers, (ii) the response produced by the molecular structure deformation, following on the diffusion of charges through percolation paths, and (iii) the dispersive response of the bound charges (dipolar response). The dipolar response presents at high frequencies one or more secondary relaxations. These processes are followed in decreasing order of frequency by the glass−rubber relaxation.

The conducting polymer−based composites are considered as heterogeneous disordered systems[11,12] and their electrical performance is directly related to the permittivity/conductivity of the all constituent's phases and to other parameters related to the filler component, as the size, shape and volume fraction of the filler. Because of the small dimensions of the filler component and the resulting high surface−to−volume ratio, composites typically have, even at low filler concentrations, a high fraction of interfacial regions (interphase) with a major influence on the electrical properties. When an electric field is applied inside a heterogeneous system, containing different constituents with dissimilar conductivities and permittivities, interfacial polarization mechanisms take place due to the accumulation of electric charges at the interfaces of

these materials. Thus, new contributions associated with the separation of charges at internal phase boundaries, referred to as Maxwell–Wagner–Sillars (MWS) polarization,[13-15] should be taking into account. The MWS effects are more pronounced for conductive materials and, in certain cases, this large–scale polarization can mask the dielectric orientation response of the material. Recently, there is evidence that this process is not unique for heterogeneous systems, since their presence has been detected in some complex homopolymers.[16-18] An example of this kind of complex homopolymers is the family of poly(n–alkyl methacrylates). Structural studies based on X–ray diffraction have shown the aggregation of side groups of different monomeric units, forming self–assembled alkyl nanodomains, their sizes being related to the length of the side group.[19,20]

For the conducting polymer–based composites, the conducting filler content results a crucial parameter that determine their electrical behavior. When the conducting filler content is low, the mean distance between conducting particles is sufficiently large and the conductivity is restricted by the presence of the dielectric matrix. However, by increasing the conductive filler content, a physical path is formed, through which the current can flow by percolating the whole system. According to the percolation theory, a transition exists from a state of limited and spatially restricted connections of conductive particles to a state of an infinite network of connections (insulator–conductor transition). The transport properties exhibit, in the vicinity of the transition, strongly non–linear behavior which in the case of electrical conduction is expressed as a power law transition.[21-24] The percolation threshold represents the critical concentration of the conductive particles content which is necessary for the onset of conductive behavior to take place.

Frequency dependent studies are very useful in order to obtain better understanding of the charge transport mechanism. In this sense, dielectric spectroscopy (DS)[9,25,26] represents a powerful tool for investigating the polymer dynamics as well as the polymer–filler interaction in composites materials. This technique allows studying the temperature and frequency dependence of the electrical conductivity. In order to investigate the physical origin of the occurring charge transport, different hopping models (the variable range hopping[27,28] and the random free–energy barrier models[29,30]) have been employed and applied to analyze the ac data.

In the present work, we report the chemical and conductive characterization of a composite with segmented polycarbonatediol polyurethane (PUPH) as matrix and commercial expanded graphite (EG) as the conducting filler. The aim of this work is the phenomenological description and interpretation of the conductivity behavior of PUPH/EG composites as a function of the expanded graphite (EG) content, temperature and frequency.

EXPERIMENTAL

Materials

Segmented thermoplastic polyurethanes are copolymers formed by hard and soft segments. In the present study, 4,4'–diphenylmethane diisocyanate (MDI), and 1,4–butanediol (BD) supplied by Aldrich (Barcelona, Spain) constituted the polyurethane hard segment and polyhexamethylene–pentamethylene carbonate diol (PH) of average molar mass 1000 supplied by UBE Chem Eur (Castellon, Spain) the soft one. Natural graphite powder lower than 20 μm size, and dimethyl acetamide

(DMAc), as solvent, were purchased from Aldrich (Barcelona, Spain). All materials are kept in a dry box to avoid humidity. Polyurethane (PUPH) solutions were obtained by a standard polymerization method based on the two–step process in DMAc.[31] Expanded graphite (EG) was obtained by the method of chemical oxidation.[32] In order to prepare the composites,[8] different weight fractions of EG between 0 and 50 wt%, were introduced in the PUPH solution. The blend was sonicated in an ultrasonic bath for 1 h, in order to disaggregate the flakes and also was vigorously stirred for 5 h to obtain a stable dispersion. The suspensions were cast on glass slides, which were previously washed in an ultrasonic bath with distilled water and later with acetone in order to eliminate the water. The polyurethane/expanded graphite composites (PUPH/EG) coated glasses were kept at 70 ºC during 12h. Films were prepared with dimensions of (4 ×2.7) cm^2 and with a thickness that ranged between 200 and 250 μm. The scheme of the chemical structure of the segmented polyurethane is shown in Fig. 1. The nomenclature used for labelling the samples, the filler content in weight and volume percentage, the glass transition temperature, T_g^{DSC}, and conductivity fitting parameters to an Arrhenius dependence are summarized in Table 1.

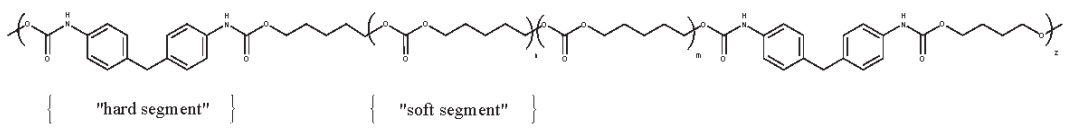

Figure 1. Scheme of the chemical structure of the segmented polyurethane in soft and hard segments.

Table 1. Sample name, composition, glass transition temperature and the corresponding values of the conductivity activation energy and pre−factor parameters of all the analyzed films.

Sample name	**Filler content by weight (%)**	**Filler content by volume (%)**	T_g^{DSC} (°C)[45]	**ln σ_0 (S cm^{-1})**	E_a^{σ} **(kJ mol^{-1})**
PUPH	0	0	-4.8	10.7±0.2	107.3±0.5
PUPH/5EG	5	2.5	-8.9	12.5±0.2	108.6±1.2
PUPH/15EG	15	8.1	-1.0	13.7±0.3	107.6±0.9
PUPH/20EG	20	11.1	-4.0	13.9±0.1	106.6±0.3
PUPH/30EG	30	17.6	-0.4	—	—
PUPH/40EG	40	25.0	-4.5	—	—
PUPH/50EG	50	33.3	-3.1	—	—

Fourier Transform Infrared Spectroscopy

Fourier transform infrared spectroscopy (FTIR) measurements were performed in a Nicolet Nexus FTIR spectrometer over the range of 450−4000 cm^{-1} with the attenuated total reflectance accessory, ATR, by co−addition of 60 scans with a spectral resolution of 2 cm^{-1}.

Raman Spectroscopy

Raman Spectroscopy analysis was performed by using a Jobin Yvon T64000 Spectrometer with a resolution of 1 cm^{-1}. The excitation source was a laser used 70−Spectrum with Ar and Kr mixture capable of producing multiple colors in the visible region. An excitation wavelength of 514 nm was used in all cases. The signal was recorded in the range of 1200 to 3000 cm^{-1}.

Morphological analysis

Scanning electron microscopy (SEM) was performed to determine the morphology on a Hitachi S−4800 microscope at an accelerating voltage of 20 kV and a working distance of 14 mm. Small pieces of samples were placed in the sample holder (aprox. 5 cm

diameter) with the aim to study the samples surface. For the cross section observation, the samples were cryoscopically fractured. All the samples were vacuum coated with a thin Au-Pd layer before testing.

X–ray characterization

The wide angle X–ray diffraction (WAXRD) was acquired on a Bruker AXS D5005 diffractometer. The samples were scanned at 4 ºC min^{-1} using Cu K_α radiation (λ = 0.15418 nm) at a filament voltage of 40 kV and a current of 20 mA. The diffraction scans were collected within the range of 2θ = 5–80º with a 2θ step of 0.01º.

Electrical Characterization

The complex impedance of PUPH and PUPH/EG composites was measured in a Novocontrol Broadband Dielectric Spectrometer (Hundsagen, Germany), integrated by a SR lock–in amplifier with an Alpha dielectric interface to carry out the measurements in the frequency range of 10^{-2}–10^6 Hz. The temperature was controlled by a nitrogen jet (QUATRO) from Novocontrol with a temperature error of 0.1 °C during every single sweep in frequency. Isothermal measurements were carried out using gold disks electrodes of 20 mm of diameter at 44 frequencies between $5 \cdot 10^{-2}$ and $3 \cdot 10^6$ Hz. PUPH and the composites until 20 wt% of EG filler were measured in the temperature range from -150 to 150 ºC (5 ºC step) while the samples with higher EG content were measured from 0 to 150 ºC (5 ºC step). The accuracy of the Alpha impedance measurements is 0.01%. The composites direct current (*dc*) conductivity, σ_{dc}, was determined from the frequency dependency of the *ac* conductivity $\sigma_{ac}(\omega)$, as the extrapolated value of the conductivity plateau in the low–frequency region.

RESULTS AND DISCUSSION

Fourier Transform Infrared Spectroscopy

Fig. 2 shows the FTIR spectra of PUPH/EG composites at different EG contents. The FTIR spectrum of the unfilled PUPH exhibits the typical bands for polyurethanes based on polycarbonatediol: N–H stretching vibration at 3200–3500 cm^{-1}, –C=O stretching vibration in the amide I region associated with free and H–bonded carbonyl groups at 1640–1800 cm^{-1}, the carbonyl C=O stretching vibration in the amide region (–NH–CO–O) at 1621 cm^{-1}, C=C aromatic stretching band at 1510 cm^{-1}, $–CH_2–$ deformation vibration at 1406 cm^{-1}, C–O carbonate group stretching band at 1226 cm^{-1}, –C–O–C– stretching band in ester group at 1056 cm^{-1} and the peak of the rolling band of the group $–CH_2–$ detected at 760 cm^{-1}. The NCO stretching band of MDI at 2270 cm^{-1} has disappeared indicating that the reaction between OH and NCO groups has been completed.[33] Polyurethanes are capable of forming several kinds of hydrogen bonds due to the presence of a donor N–H group and a C=O acceptor group in the urethane linkage. This is why hard segment–hard segment or hard segment–soft segment hydrogen bonding can exist. In the case of polycarbonatediol–polyurethane, the appearance of a N–H band at 3310 cm^{-1} and a small one at 3000 cm^{-1} are attributed to "free" and H–bonded N–H groups, respectively. These bands decrease with the EG content suggesting that the filler disrupt the ordered structure of hard–hard and hard–soft interactions. On the other hand, the stretching vibration of the C=O groups in the hard segments[34] give rise to: (i) a main peak centered at 1735 cm^{-1}, associated with C=O groups that are free (non–hydrogen bonded); and (ii) the peak at 1700 cm^{-1} that resulted from hydrogen bonding with urethane N–H groups. Significant suppression in

hydrogen bonding can be inferred from the diminished peak intensity at 1700 cm^{-1} as the amount of EG increases. These results suggest that the carboxyl groups in EG contribute to the interfacial interaction between the PUPH backbone and the EG layers. In other words, the C=O groups of the hard segments of PUPH may form hydrogen bonds with the hydroxyl groups of few–layered graphene. It is observed a decrease in the intensity of 1730 cm^{-1} and 1700 cm^{-1} bands when the EG concentration is higher than 15 wt%, being this decrease more noticeably for the last one. This fact implies that addition of EG disrupt the carbonyl interactions indicating a good dispersion of the EG in the thermoplastic polyurethane. Furthermore, the difficulty to detect the characteristics' signals of PUPH chains with increasing the EG content could be related to the existence of some type of tether between both components.

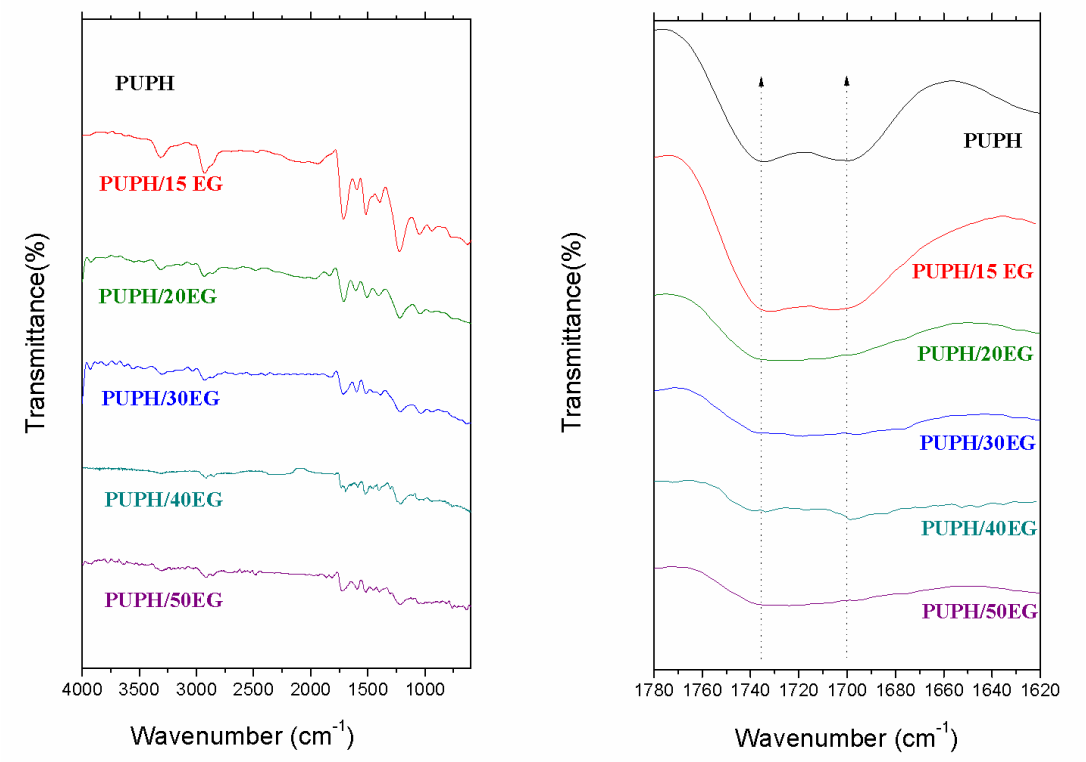

Figure 2. FTIR spectra for PUPH and PUPH100/EG composites. The spectra were scaled in the carbonyl absorbance region for better visualization.

Raman Spectroscopy

Raman spectroscopy is commonly used to study the degree of exfoliation and the structure perfection of the expanded graphite, easier detectable at low EG content because the technique is highly sensitive to the density of defects and to the number of graphene layers.[35] Fig. 3 shows the Raman Spectra of PUPH, EG and PUPH/EG composites with 0 to 50 wt% of EG content recorded by using a laser excitation wavelength of 514 nm in the region of 1200–3000 cm^{-1}. The polyurethane spectrum shows the characteristic bands indicated as follows: the bending of C–H at 1308 cm^{-1}, the asymmetric stretching of N=C=O and the bending mode of CH_2 at 1445 cm^{-1}, the stretching of C–N and the bending of N–H at 1530 cm^{-1}, the peak related to aromatic ring breathing/stretching vibrational modes present in the phenylene groups of MDI appears at 1612 $cm^{-1}$and finally the CH_2–CH_3 vibrational modes at 2800–3000 cm^{-1}.[36] Three characteristic bands are observed for pristine expanded graphite. The D–band (defect–induced mode) at 1353 cm^{-1} appears when disorder is present in carbon aromatic structure. The G–band (E_{2g} mode) located at 1580 cm^{-1} is one of the carbon materials bands attributed to the doubly degenerate vibration corresponding to the hexagonal E_{2g} mode of graphite with symmetry D^4_{6h}.[37] The G'–band (second–order band) at 2600–2800 cm^{-1} is observed in all carbonaceous materials. It is the second harmonic (or overtone) of the D–band due to the presence of sp^2 bonded carbon atoms. For the PUPH/EG composites, the D–band is only detected at compositions higher than 40 wt%, and the G– and G'–band at compositions higher than 20 wt%. In order to quantify the interaction degree between PUPH and EG the spectra were fitted to Lorentz curves to determine the areas of the corresponding bands, I_D and I_G. The ratio between

the areas of the D–band to the G–band (I_D/I_G) can be related to the order in carbonaceous materials.[38] The I_D/I_G ratio has been calculated for EG and PUPH/50EG because at compositions below 50 wt% of EG the D–band is not well resolved. The ratio I_D/I_G in the sample with 50 wt% of EG is 0.07, lower than the corresponding to pristine EG (0.16). This fact indicates that the polymer chains have a negative effect in the alignment of the graphite particles.

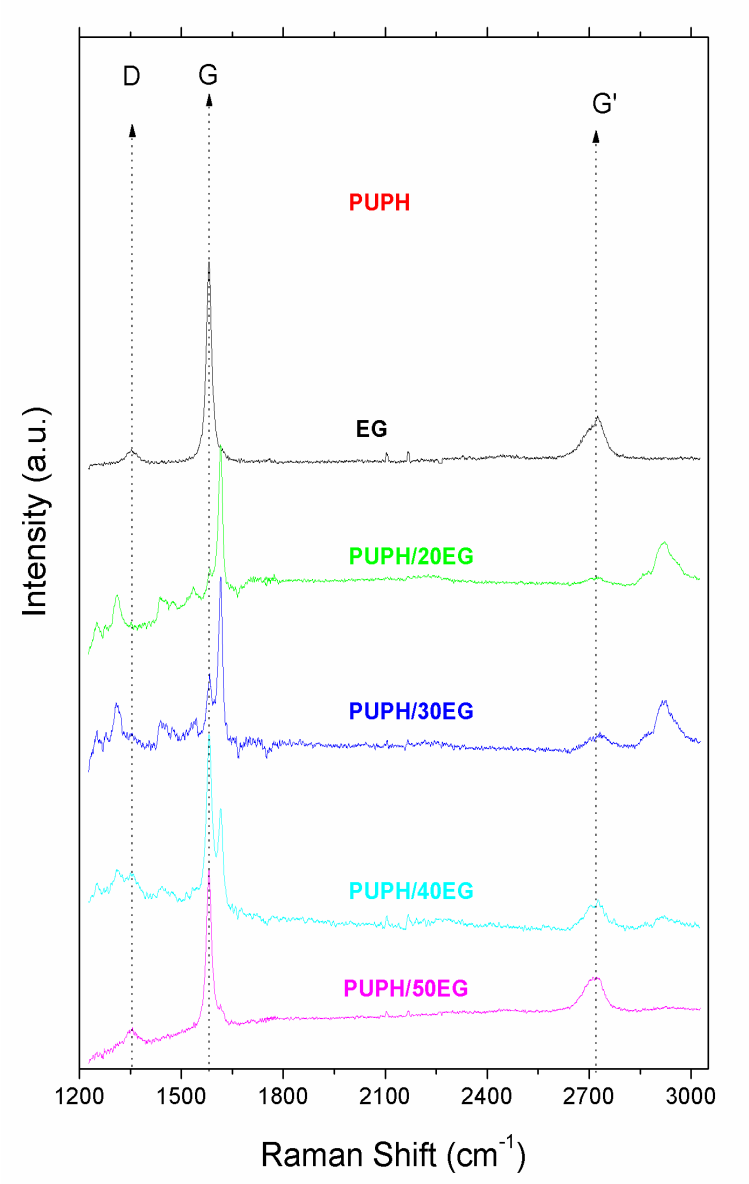

Figure 3. Raman Spectra of PUPH, EG and PUPH/EG composites. The spectra were scaled for better visualization.

Morphological analysis

Fig. 4 shows SEM images of EG, PUPH, PUPH/15EG, and PUPH/50EG. Graphite is formed by carbon atoms sp^2 bonded in flat planes that keep together due to Van der Waals forces. Graphite can be intercalated with a convenient solvent, as in this work, and later with fast heating to a high temperature leads to exfoliation consisting of an increase in the dimension perpendicular to the carbon layers of the intercalated graphite. Expanded graphite, as shown in Fig. 4(A), shows a structure based on parallel boards resulting in many pores. The spacing between the graphite layers increases during exfoliation giving a porous structure consisting of numerous graphite sheets, so that the polymer can be easily intercalated among them. Figs. 4(B), 4(D) and 4(F) show the surface of the PUPH/EG composites with 0, 15 and 50 wt% EG content, respectively. Obviously, in contrast to the PUPH surface, a certain roughness was appreciated in presence of expanded graphite. This is evident when comparing the last two images, being the roughness higher in the sample with higher EG content. Figs. 4(C), 4(E) and 4(G) correspond to the cross section of the PUPH, PUPH/15GE and PUPH/50EG films, respectively. A good affinity of the EG for the PUPH is observed as the EG layers become absorbed by the polyurethane leading to a continuous composite structure.

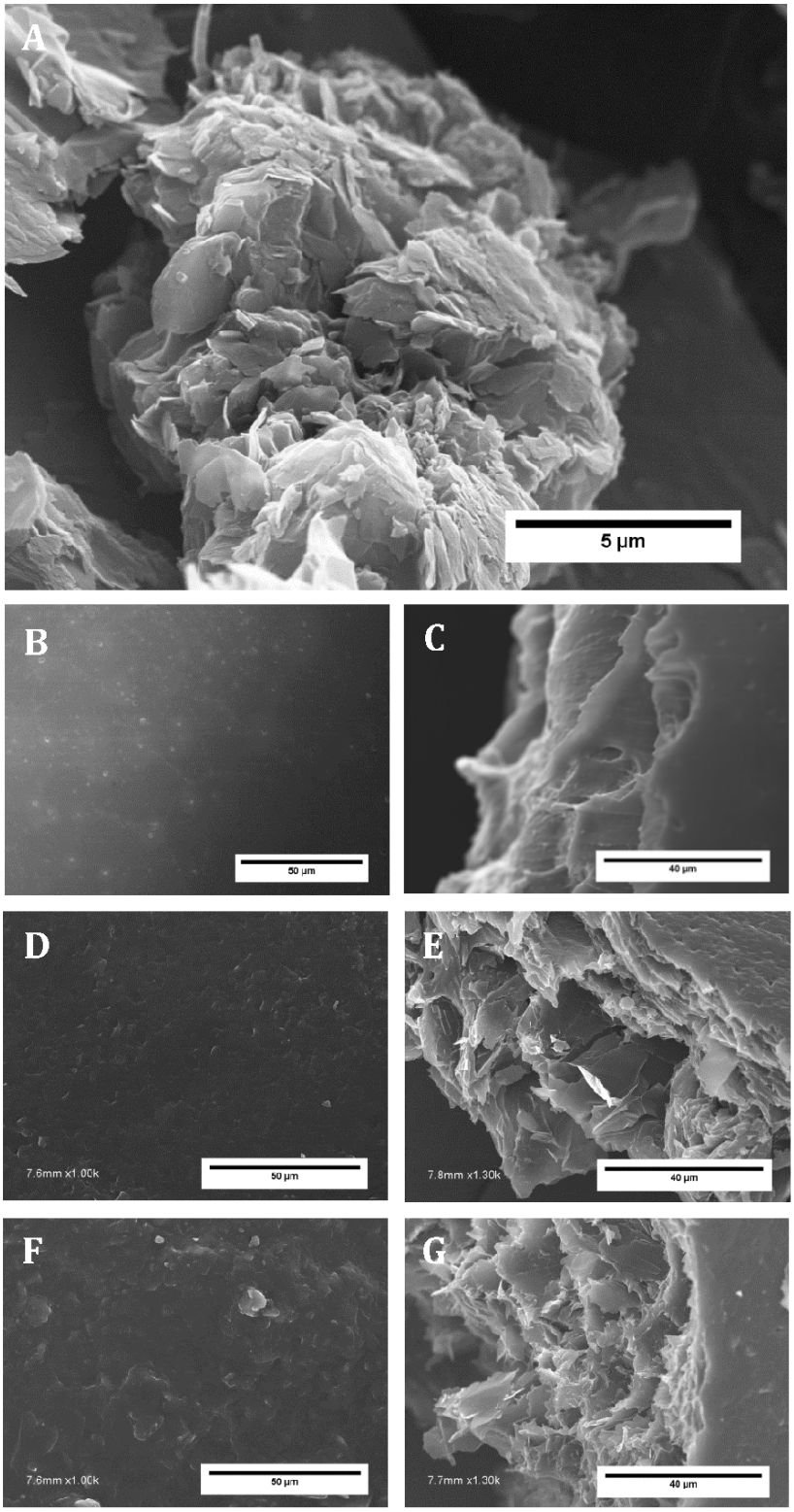

Figure 4. SEM images of: EG (A); PUPH (B), PUPH/15EG (D) and PUPH/50EG (F) are surface images; and PUPH (C), PUPH/15EG (E) and PUPH/50EG (G) are a cross section of the cryoscopic fracture.

X–ray characterization

Fig. 5 shows the X–ray patterns of EG, PUPH and PUPH/EG composites. EG shows a two sharp peaks at q=18.7 nm^{-1} (2θ=26°) corresponding to diffraction in the (002) plane and at q=37.5 nm^{-1} (2θ=54°) corresponding to the diffraction in the (110) plane.[39] The spectrum of PUPH shows the presence of a broad peak centered in the vicinity of q=14.5 nm^{-1} (2θ=20.65°) and a small shoulder at q=8.9 nm^{-1} (2θ=12.6°). These peaks are ascribed to the micro–phase separated morphology into "soft" and "hard" segments occurring during polymerization and are an indication of short range order, commonly observed in polyurethanes.[40] The composites show a narrow diffraction peak at q=18.7 nm^{-1} (2θ=26°) associated with the EG filler. The intensity of the peaks related to PUPH at 2θ=20.65° decreases significantly, whereas that at 2θ=12.6° increases with the addition of EG. The intensity reduction reflects, in some way, an eventual reduction in the number of existing nanodomains in the film. The interdomain spacing d, which only depends on the molecular weight of the macrodiol was estimated using the Bragg's law to be equal to 0.5 nm.

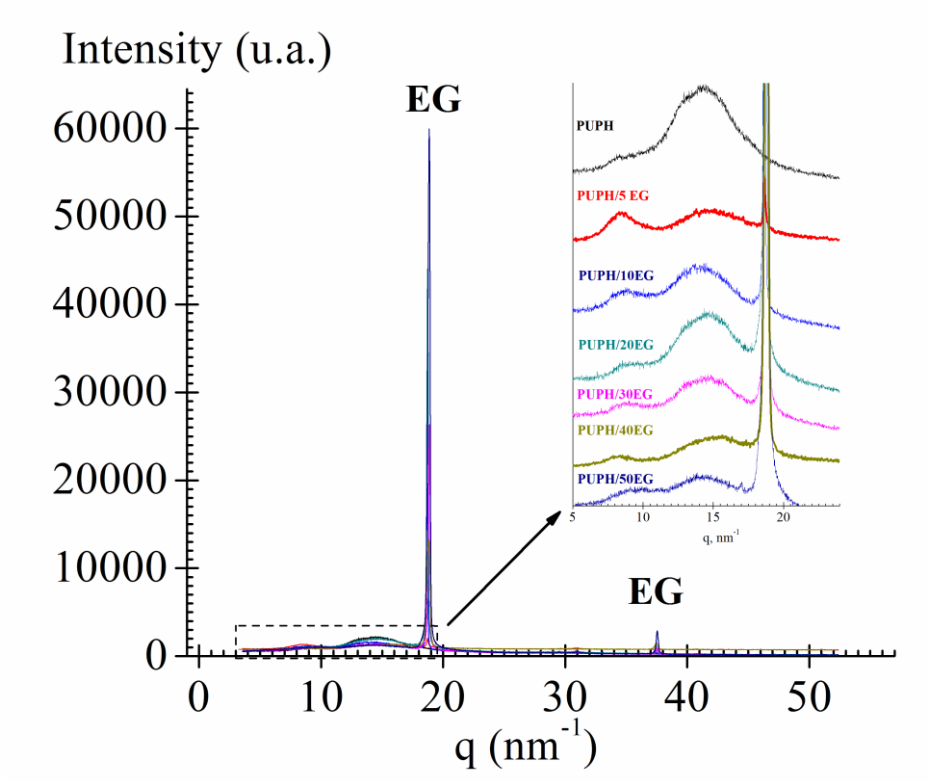

Figure 5. X–ray diffraction patterns of EG, PUPH and PUPH/EG composites at different EG contents. Inset: zoom of the X–ray pattern in the 0 to 20 nm^{-1} region. The spectra were scaled for better visualization.

Electrical Characterization

Fig. 6 shows the temperature dependence of the dielectric permittivity and loss factor at 1 kHz, for the pure PUPH and the PUPH/EG composites. As we can observe, both the dielectric permittivity and loss factor, exhibit an abrupt variation by adding a 30 wt% of EG filler. For lower EG contents, the segmental dynamics of the PUPH matrix seems to be slightly affected by the presence of the EG filler, which is in agreement with previous observations reported for other composites.[41,42]

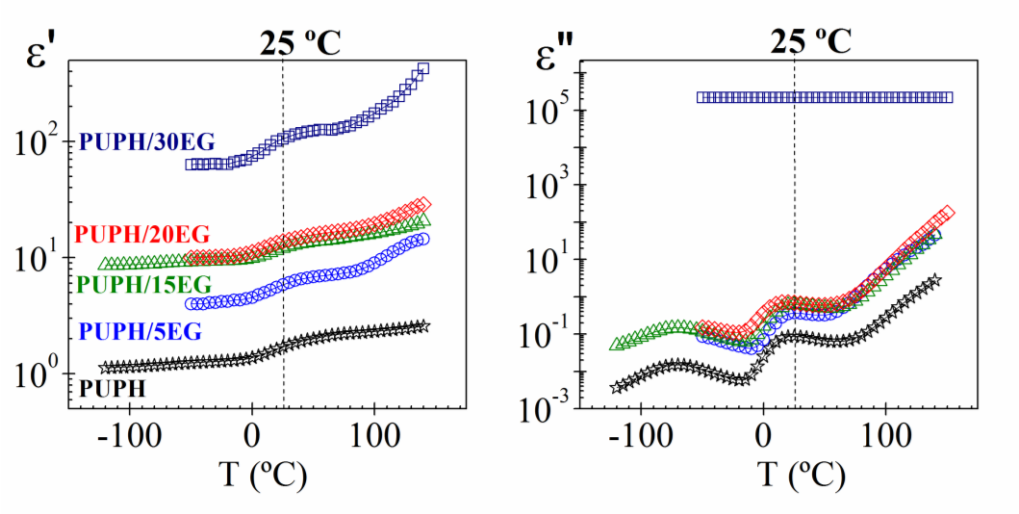

Figure 6. Temperature dependence of the complex permittivity, at 1 kHz, for PUPH (●) and PUPH/EG composites with different EG weight fractions (wt%).

The complex dielectric permittivity $\varepsilon^*(\omega)=\varepsilon'(\omega)-i\cdot\varepsilon''(\omega)$, and complex electrical conductivity, $\sigma^*(\omega)=\sigma'(\omega)+i\cdot\sigma''(\omega)$ are related to each other by $\sigma^*(\omega)=i\cdot\omega\cdot\varepsilon_0\cdot\varepsilon^*(\omega)$, where ε_0 is the vacuum permittivity. So, the real and imaginary part of $\sigma^*(\omega)$ are given, respectively, by $\sigma'(\omega)=\sigma'_{ac}(\omega)=\omega\cdot\varepsilon_0\cdot\varepsilon''(\omega)$ and $\sigma''(\omega)=\omega\cdot\varepsilon_0\cdot\varepsilon'(\omega)$.

Fig. 7 shows in double logarithmic plots the real component of the complex conductivity, $\sigma'=\sigma_{ac}$ (S cm^{-1}), in the frequency domain for pure PUPH, and PUPH/EG composites, measured at several temperatures. According to Fig. 7, the dc conductivity of the analyzed samples increases with increasing temperature and EG content. The conductivity exhibits a frequency dependence which becomes stronger as the concentration of EG decreases. For low EG content, it is evident that the ac conductivity, $\sigma_{ac}(\omega)$ increases with frequency and temperature, being dependent of both magnitudes. The change of the conductivity at high frequencies is due to the increasing importance of the polarization effects on the macroscopic conductivity. As usual, in the

frequency domain, the isotherms corresponding to high temperatures exhibit a plateau in the low frequency region, reflecting a frequency independent conductivity, *i.e.*, dc conductivity. The frequency range covered by the plateau increases with temperature. The bulk conductivity of the pure PUPH increases with increasing frequency, as expected for an insulator material, with a value at 30 ºC and 10^{-1} s^{-1} of about $2 \cdot 10^{-14}$ S cm^{-1}. The conductivity value of the PUPH sample increases to ~ $4 \cdot 10^{-10}$ S cm^{-1} at 120 ºC and 10^{-1} s^{-1}, that is, four orders of magnitude. As we can observe, for samples with EG content less or equal to 20 wt%, the frequency dependence of $\sigma'(\omega)$ is nearly linear [$\sigma'(\omega) \sim \omega^{s}$] in the high frequency range. However, for EG content equal or higher than 30 wt%, a frequency independent conductivity is obtained in all the experimental frequency range. This absence of a frequency dependence for high EG contents could be related to the occurrence of a highly interconnected filler network with almost the absence of electrical barriers. We can also observe that the dc conductivity significantly increases for EG content equal to or higher than 30 wt%. This observation suggests that the critical filler content, *i.e.*, the percolation threshold, should be near 30 wt% for this particular PUPH/EG composite series. The MWS process is related to the build–up of charges at the interfaces of components of heterogeneous systems. The charges can migrate under the influence of the applied field contributing to the electrical response of the systems.[43,44] In our case, this phenomenon is related to the micro–phase separation of the "soft" and "hard" segments. The reduction of the MWS process definition with the EG content reflects a probable reduction in the number of existing nanodomains imposed by the EG filler. This result is in agreement with that of X–ray. Thus, the incorporation of EG filler governs the polymer chain movement and, consequently, the molecule polarization, which it is reflected in the dielectric spectra by the reduction of

the MWS process intensity.

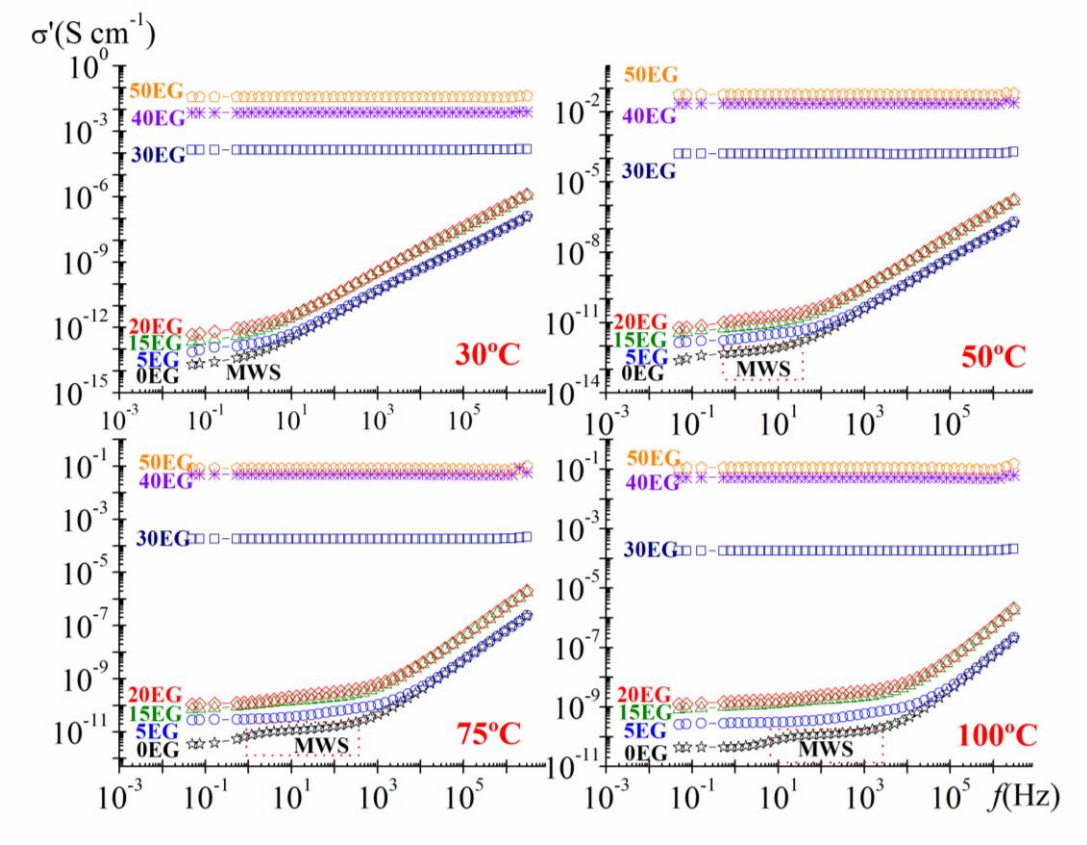

Figure 7. Frequency dependence of the ac conductivity, at several temperatures, for pure PUPH polymer and PUPH/EG composites films, with an EG weight fraction (wt%).

In order to study the effect of the EG content on the electrical conductivity of PUPH/EG composites, we have represented in Fig. 8 the electrical conductivity σ_{ac} as a function of the EG weight percentage. As we can observe, the conductivity increases continuously with the EG content in all the studied temperatures. Moreover, for constant conductive filler content, a considerable increase of the conductivity appears as the temperature is raised. According to these results, the temperature dependence of the conductivity is more significant for EG contents lower than 30 wt%. The increase of EG content results beneficial to form conductive. By further addition of EG filler the

conductivity is gradually improved, and a sharp transition occurs at EG content of 30 wt%. Finally, for EG content higher than 40 wt%, non–significant changes are observed in the conductivity values.

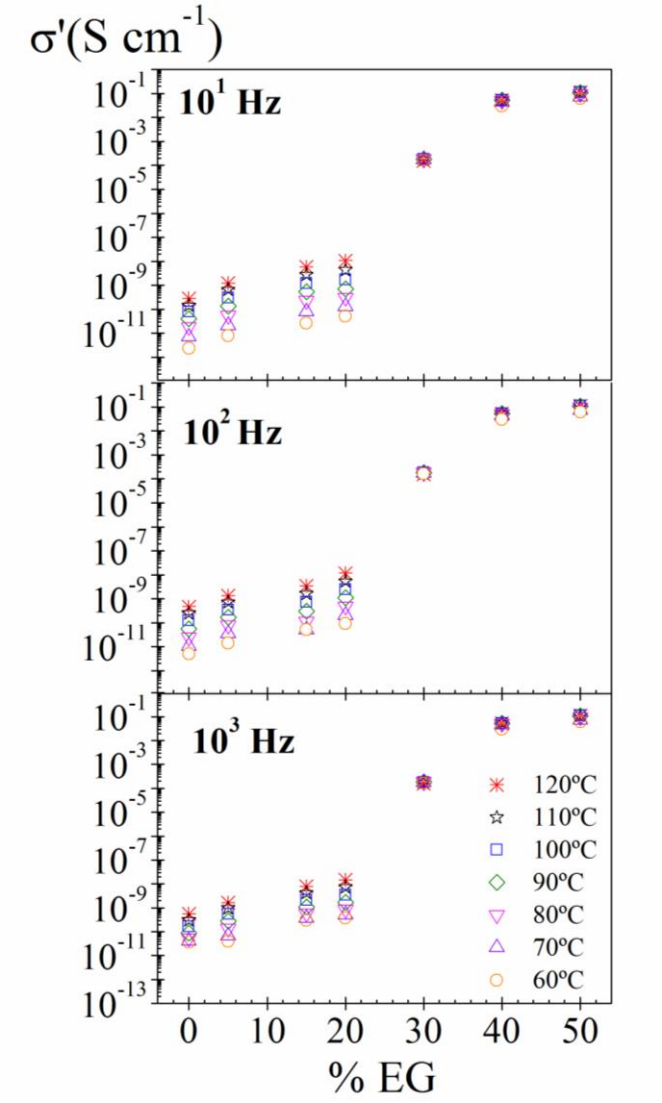

Figure 8. The EG content dependence of the conductivity for PUPH/EG composites at various temperatures between 60 and 120 ºC at several frequencies: 10^3, 10^2 and 10^1 Hz.

Fig. 9 shows dc conductivity at 30 and 140 ºC, evaluated from the $\sigma'(\omega)$ value when $\omega \rightarrow 0$, as a function of the EG mass fraction. At both temperatures a sharp

increase in the electrical conductivity is observed when the EG content reaches 30 wt%. This increase is more pronounced at 30ºC.

In order to calculate the percolation threshold, the data were fitted to the scaling law of the percolation theory. This theory defines an insulation–conductor transition and a corresponding threshold of the conductive filler concentration via the equation:[44-46]

$$\sigma_{dc} = C \cdot \left(p - p_c \right)^t \qquad p > p_c \tag{1}$$

where C is a constant, p_c is the weight fraction of filler or percolation threshold and t is the scaling critical exponent. The critical t exponent is related to the dimensionality of the system (1.3 and 2 in two and three dimensional materials, respectively).[47] The data were fitted to the scaling law and the values of C, p_c and t, evaluated by multiple non–linear regression analysis, are listed in Table 2.

According to our results, the percolation threshold, p_c, is nearly temperature independent (Figure 8). Thus, the p_c values obtained for both analyzed temperatures are very similar. Moreover, these values are higher than those reported for other composites with EG [48]. This fact is directly related to the morphology of the filler, which clearly depends on the processing conditions[49,50].

Furthermore, the scaling critical exponent, t, decreases slightly with the temperature and the obtained value is somewhat smaller than the universal value of three–dimensional percolating systems (t = 2). The increase of t with decreasing temperature could be then associated with the reduction in the dimensionality of the conductive network, which occurs when temperature increases.

In all composites analyzed, the conductivity did not exceed 10^{-1} S cm^{-1}, which is 13 orders of magnitude higher than PUPH, but much lower than the corresponding to

EG filler. Moreover, extrapolation to p=100% using Eqn.(1) gives a conductivity of 0.32 and 0.73 S cm^{-1} for 30 ºC and 140 ºC, respectively. These values are 3 orders of magnitude lower than the conductivity measured in EG pure filler.[51] This result could be related to the coating of the individual EG particles by the PUPH insulating surface, resulting in a poor electrical contact between the EG particles. Therefore for low EG content, the matrix acts as an electrical barrier, avoiding the direct contact between the EG particles.

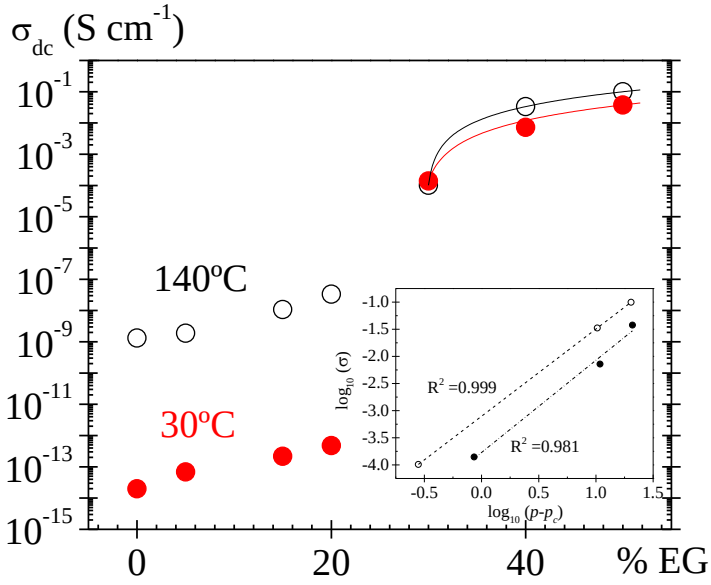

Figure 9. Dependence of the dc conductivity on the EG weight mass fraction, p, at 30 ºC and 140 ºC (1 kHz). The solid line is a fit to the scaling law of the percolation theory.

Table 2. Percolation scaling law parameters at 30 ºC and 140 ºC.

	30 ºC	**140 ºC**
t	1.76±0.01	1.61±0.01
***p*$_c$ (wt%)**	29.14±0.02	29.72±0.02
***C* (S cm^{-1})**	$1.82\cdot10^{-4}\pm1.07\cdot10^{-13}$	$7.88\cdot10^{-4}\pm1.37\cdot10^{-8}$

Fig. 10 shows the dc conductivity values, obtained at several temperatures from extrapolations to low frequencies, as a function of the reciprocal ~~of~~ temperature for all the examined composites. As we can see, the dc conductivity is a thermally activated process and can be described by $\sigma_{dc} = \sigma_0 \cdot \exp(-E_a/RT)$. The experimental data were satisfactorily linear fitted to an Arrhenius plot, and the evaluated activation energy (E_a) and pre–factor (σ_0) values are summarized in Table 1. According to our results, the reduction of the inter–particle separation, by increasing the weight mass fraction of the EG, results in the reduction of the corresponding activation energy values.

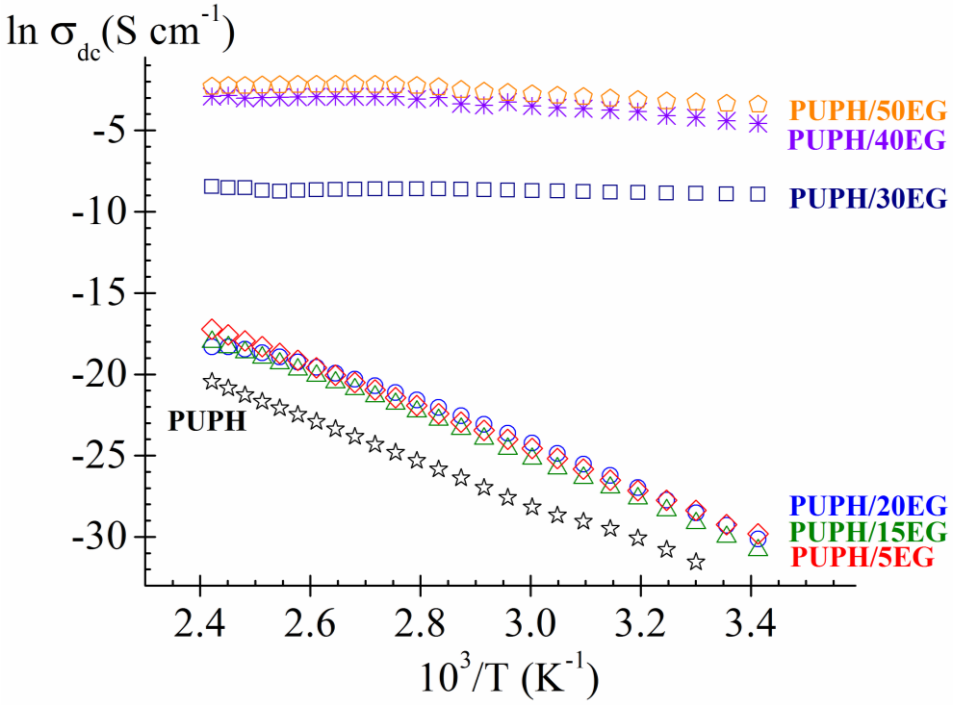

Figure 10. Plot of neperian logarithmic of the dc conductivity as a function of the reciprocal temperature.

CONCLUSIONS

Composites of polycarbonatediol polyurethane and expanded graphite have been

synthesized with different EG compositions, mainly to study ~~the~~ its electrical conductive/dielectric behavior. FTIR and Raman spectroscopies, X–Ray diffraction and SEM of the composites indicate a good average dispersion of EG in the polyurethane matrix with good filler–polymer interactions.

The electrical conductivity and dielectric properties of PUPH/EG composites were studied in a wide range of frequencies and temperatures. These measurements show that the dielectric permittivity and electrical conductivity of the composites increase with the addition of EG, as expected. An insulator–to–conductor transition is observed with the EG content. Thus, an abrupt variation of both, dielectric permittivity and ac conductivity, is observed at EG content near to 30 wt%. Only in the PUPH sample or in the low EG content compositions, the interfacial polarization or MWS process, is good defined. This result, together with the X–ray analysis, indicates that the EG produces a reduction in the number of formed nanodomains, directly responsible of this conductive process.

For low contents of EG conducting filler (10–20 wt%), the conductivity of the composites is temperature and frequency dependent and remains at the level of the polymeric PUPH matrix (~10^{-14} S cm^{-1}). As the EG filler content increases, a critical concentration of p_c~30wt% is reached. Above this p_c it is observed that conductivity is nearly frequency and temperature independent and a sharp increase, of several orders of magnitude, takes place. From these results it can be concluded that the conduction comes about percolation paths. The percolation theory has been used to describe the insulator–to–conductor transition.

Finally, the existence of percolation paths at high EG content it is also supported by the observed Arrhenius conductivity behavior and by the activation energy dependence on the EG content. The higher activation energy values observed for the low filler contents can be rationalized if we consider that the mean distance between filler particles increases with decreasing filler content.

ACKNOWLEDGEMENTS

This work was financially supported by the DGCYT through Grant MAT2012−33483.

The authors thank UBE Chem Corporation for supplying the polycarbonatodiol to synthesize the polyurethanes of this work.

REFERENCES

1 Pascault JP, Satereau H, Verdu J, Williams RJJ (Eds) *In Thermosetting Polymers*, Marcel Dekker, New York, USA, (2002)

2 Pinnavaia TJ, Bell GW (Eds), *Polymer–clay Nanocomposites*, Wiley, New York USA, (2000).

3 Zhu Y, Xiong J, Tang Y, Zuo Y, *Progress in Organic Coatings* **69**: 7–11 (2010).

4 Garcia-Pacios V, Costa V, Colera M, Miguel Martin-Martinez J, *Progress in Organic Coatings* **71**: 136–146 (2011).

5 Sandu I, Brasoveanu M, Morjan I, Voicu I, Dumitrache F, Teodor CF, Gavrila-Florescu L, *Thin Solid Films* **519**: 4128–4131 (2011).

6 Konwer S, Maiti J, Dolui SK, *Materials Chemistry and Physics* **128**: 283–290 (2011).

7 He F, Fan J, Lau S, *Polymer Testing* **27**: 964–970 (2008).

8 Gómez CM, Culebras M, Cantarero A, Redondo–Foj B, Ortiz–Serna P, Carsí M, and Sanchis MJ, *Appl Surf Sci* **275**:295–302 (2013).

9 Kremer F, Schönhals A*In Broadband Dielectric Spectroscopy*, Springer, Berlin, (2003).

10 Carsí M, Sanchis MJ, Ortiz–Serna P, Redondo–Foj B, Díaz–Calleja R and Riande E, *Macromolecules* **46:**3167–3175 (2013).

11 Strümpler R and Glatz–Reichenbach J, *J. Electroceram* **3(4)**:329–346 (1999)

12 Dyre JC, Schrøder TB, *Rev. Modern Phys* **72(3)**:873–892 (2000).

13 Maxwell J. C. *Electricity and Magnetism* , Clarendon Oxford, U.K, (1893).

14 Wagner KW, *Arch Electrotech* **2**:371–387 (1914).

15 Sillars RW, *Inst Elect Eng* **80**:378-394 (1937).

16 Arbe A, Genix AC, Arrese–Igor S, Colmenero J and Richter D, *Macromolecules* **43**:3107–3119 (2010).

17 Sanchis MJ, Carsí M, Ortiz–Serna P, Domínguez–Espinosa G, Díaz–Calleja R, Riande E, Alegría L, Gargallo L and Radic D, *Macromolecules* **43**:5723–5733 (2010).

18 Hempel E, Beiner M, Huth H and Donth E *Thermochim. Acta* **391(1)**:219–225 (2002).

19 Beiner M, *Rapid Comm* **22(12)**:869–895 (2001).

20 Beiner M and Huth H, *Nat Matter* **2(9)**:595–599 (2003).

21 Zallen R, *The Physics of Amorphous Solids*, Wiley, New York, chapter 4, (2004).

22 Bunde A, Havlin S. *Fractal and disordered systems*, Springer–Verlag Berlin, chapters 2-3, (1991).

23 Stauffer D. *Introduction to percolation theory*, Taylor & Francis London (1984).

24 Lux F, *J. Mater* Sci **28(2)**:285–301 (1993).

25 McCrum NG, Read BE and Williams W, *Anelastic and Dielectric Effects in Polymeric Solids*, Dover Publications, Inc.New York, p. 118, (1991).

26 Riande E, Díaz Calleja R. *Electrical Properties of Polymers*, Marcel Dekker Inc.New York, (2004)

27 Mott NF, *Metal insulator transitions*, Taylor & Francis London, (1990).

28 Mott NF. *Conduction in non-crystalline materials*, Clarendon Press Oxford, (1987).

29 Dyre JC, *J Appl Phys* **64(5)**:2456–2468 (1988).

30 Dyre JC and Schrøder TB, *Phys Stat Sol B* **230(1-3)**:5–13 (2002).

31 Costa V, Nohales A, Félix P, Guillem C and Gómez CM, *Journal of Elastomers & Plastics* **45(3)**:217-238 (2012).

32 Dhakate SR, Sharma S, Borah M, Mathur RB and Dhami TL, *International Journal of Hydrogen Energy* **33(13)**:7146–7152 (2008).

33 Meuse CW, Yang X, Yang D and Hsu SL, *Macromolecules* **25(2)**:925–932 (1992).

34 Seymour RW, Allegrezza AE and Cooper SL, *Macromolecules* **6(6)**:896–902 (1973).

35 Gupta A, Chen G, Joshi P, Tadigadapa S and Eklund PC, *Nano Lett* **6(12)**:2667–2673 (2006).

36 Parnell S, Min K and Cakmak M, *Polymer* **44(18)**:5137–5144 (2003).

37 Heise HM, Kuckuk R, Ojha AK, Srivastava A, Srivastava V and Asthana BP, *J Raman Spectrosc* **40(3)**:344–353 (2009).

38 Culebras M, Madroñero A, Cantarero A, Amo J, Domingo C and López A, *Nanoscale Research Letters* **7**:588 (2012).

39 Li ZQ, Lu CJ, Xia ZP, Zhou Y and Luo Z, *Carbon* **45(8)**:1686–1695 (2007).

40 Ryan AJ, Macosko CW and Bras W, *Macromolecules* **25(23)**:6277–6283 (1992)

41 Cangialosi D, Boucher VM, Alegría A and Colmenero J, *Polymer* **53**:1362 (2012).

42 Otegui J, Schwartz GA, Cerveny S, Colmenero J, Loichen J and Westermann S, *Macromolecules* **46(6)**:2407–2416 (2013).

43 Psarras GC, *Composites Part A: Appl Sci Manufact* **37(10)**:1545–1553 (2006).

44 Aharony A, Stauffer D. *Introduction to percolation Theory*, Taylor and Francis London: 2nd Edition, (1993).

45 Krupa I and Chodák I, *Eur Polym J* **37(11)**:2159–2168 (2001).

46 Novák I, Krupa I and Chodák I, *J. Mat Sci Letters* **21**:1039–1040 (2002).

47 Lux F, *J. Mater Sci* **28(2):**285–301 (1993).

48 Chao Li Y, Yiu Li RK, Chin Tjong S, *Journal of Nanomaterials* **2010:** ID 261748 (2010).

49 Piana F, Pionteck J, *Composites Science and Technology* **80:** 39-46 (2013).

50 Eceiza, Larrañaga M, de la Caba K, Kortaberria G, Marieta M, Corcuera MA, Mondragon I, *Journal of Applied Polymer Science* **108:** 3092-3103 (2008).

51 Marinho B, Ghislandi M, Tkalya E, Koning CE and de With G, *Powder Technology* **221**:351–358 (2012).

Figure Caption

Figure 1. Scheme of the chemical structure of the segmented polyurethane in soft and hard segments.

Figure 2. FTIR spectra for PUPH and PUPH100/EG composites. The spectra were scaled in the carbonyl absorbance region for better visualization.

Figure 3. Raman Spectra of PUPH, EG and PUPH/EG composites. The spectra were scaled for better visualization.

Figure 4. SEM micrographs of EG (A), PUPH (B and C), PUPH/15EG (D and E) and PUPH/50EG (F and G).

Figure 5. X–ray diffraction patterns of EG, PUPH and PUPH/EG composites at different EG contents. Inset: zoom of the X-ray pattern in the 0 to 20 nm^{-1} region. The spectra were scaled for better visualization.

Figure 6. Temperature dependence of the complex permittivity, at 1 kHz, for PUPH (●) and PUPH/EG composites with an EG weight fraction (wt%) of 5 (○), 15 (▲), 20 (Δ) and 30 (■).

Figure 7. Frequency dependence of the ac conductivity, at several temperatures, for pure PUPH polymer (●) and PUPH/EG composites films, with an EG weight fraction (wt%) of 5 (○), 15(▲), 20 (Δ), 30 (■), 40 (□) and 50 (▼).

Figure 8. The EG content dependence of the conductivity for PUPH/EG composites at various temperatures between 60 ºC and 120 ºC at 10^3, 10^2 and 10^1 Hz.

Figure 9. Dependence of the dc conductivity on the EG weight mass fraction, *p*, at 30 ºC and 140 ºC (1kHz). The solid line is a fit to the scaling law of the percolation theory.

Figure 10. Plot of neperian logarithmic of the dc conductivity as a function of reciprocal temperature.